PROCEEDINGS OF SCIENCE

Review of recent Heavy Ion Physics results at the LHC

Luigi Dello Stritto[a,*]

[a] *CERN*

E-mail: luigi.dello.stritto@cern.ch

Heavy-ion collisions at the Large Hadron Collider (LHC) offer a unique laboratory for probing the quark-gluon plasma (QGP), a novel state of matter believed to have existed shortly after the Big Bang. In this contribution, the latest findings from the LHC, focusing on key observables that shed light on various aspects of the QGP, are presented. Heavy-flavor hadrons and jet observables, such as jet quenching and broadening, provide crucial insights into the interactions between high-energy partons and the QGP, probing the medium energy density and transport properties. The study of quarkonia suppression, in both ground and excited states, reveals the binding dynamics of heavy quarks within the plasma, while flow patterns offer evidence of the thermalization of the QGP and of collective behavior. Additionally, direct photons serve as penetrating probes, delivering unaltered information from the early stages of the collision, and allowing for the determination of the medium initial temperature and fundamental characteristics. Recent studies of rare processes via ultra-peripheral collisions (UPC) are also discussed. By integrating these diverse findings, a broad overview of the current state of heavy-ion physics research at the LHC is provided.

The 43rd International Symposium on Physics in Collision
22-25 October 2024
NCSR "Demokritos", Athens, Greece

*Speaker

© Copyright owned by the author(s) under the terms of the Creative Commons Attribution-NonCommercial-NoDerivatives 4.0 International License (CC BY-NC-ND 4.0) All rights for text and data mining, AI training, and similar technologies for commercial purposes, are reserved. ISSN 1824-8039 . Published by SISSA Medialab.

PoS(PIC2024)046

1. Introduction

Heavy-ion collisions at the LHC play a pivotal role in advancing our understanding of fundamental physics. These collisions create extreme conditions of temperature and density, similar to those present in the early universe, providing a unique environment to test Quantum Chromodynamics (QCD) predictions under such extremes. In these conditions, standard hadronic matter is expected to melt, transitioning into a novel state of deconfined color charges known as the quark-gluon plasma (QGP). The primary objective of heavy-ion collision studies is to investigate the formation and properties of the QGP. However, these collisions also open the door to other valuable avenues of research. One such area involves ultra-peripheral collisions (UPC), where nuclei interact at very large impact parameters. In UPCs, the nuclei do not physically collide but pass close enough for their electromagnetic fields to interact, creating a clean environment for exploring rare processes. Recent measurements on the heavy-ion collision data collected at the LHC by the ATLAS [1], CMS [2], ALICE [3], and LHCb [4] experiments are discussed in this paper.

2. Probing the quark-gluon plasma

High-energy heavy-ion collisions provide the conditions necessary to reach the critical temperature for a phase transition, resulting in the formation of QGP. The medium subsequently thermalizes and begins to expand. During this expansion, it undergoes cooling, and once the temperature drops below the critical threshold, the system hadronizes. This entire process occurs within a few femtoseconds ($10^{-15}s$), making it an extremely rapid phenomenon. Given the transient nature of QGP, its properties cannot be studied directly. Instead, its investigation relies on indirect signatures inferred from the stream of free particles detected after hadronization.

One of the key signatures of QGP formation is the emergence of collective motion, or flow, among the particles produced in the collision. This flow reflects the hydrodynamic expansion of the hot, dense medium created in the collision, providing valuable insights into the QGP properties. The collective behavior of particles is strongly influenced by the initial conditions of the collision, including the asymmetric geometry of the colliding nuclei. These initial conditions give rise to spatial anisotropies in the final particle distributions observed in detectors. These anisotropies are typically studied by expanding the particle distribution in momentum space into a Fourier series with respect to the reaction plane, defined by the beamline and the impact parameter vector (eq. 1).

$$\frac{dN}{d\phi} = \frac{N}{2\pi}[1 + 2\sum_{n=1}^{\infty} v_n \, cos(n(\phi - \Psi_{RP})] \tag{1}$$

The Fourier coefficients v_n, or flow harmonics, quantify anisotropies in the QGP. The second harmonic (elliptic flow) reflects the initial collision geometry, while higher-order harmonics stem from event-by-event energy density fluctuations. These harmonics reveal key QGP properties, such as viscosity, collectivity, and thermalization dynamics The elliptic flow of charged particles has been measured by ATLAS [5], ALICE [6], and LHCb [7] in two different centrality ranges and it is shown in Fig. 1. The results from ALICE and ATLAS exhibit excellent agreement, while LHCb measurements indicate slightly lower elliptic flow values. This discrepancy aligns with expectations, as LHCb probes a different pseudorapidity range where collective effects are

PoS(PIC2024)046

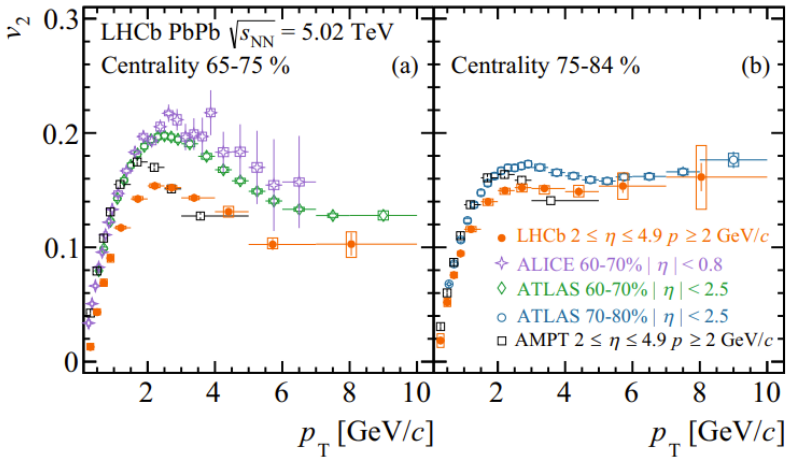

Figure 1: Second-flow harmonic coefficients as function of p_T measured by ATLAS [5], ALICE [6], and LHCb [7] Collaborations. LHCb measurements are compared with the AMPT model predictions [8].

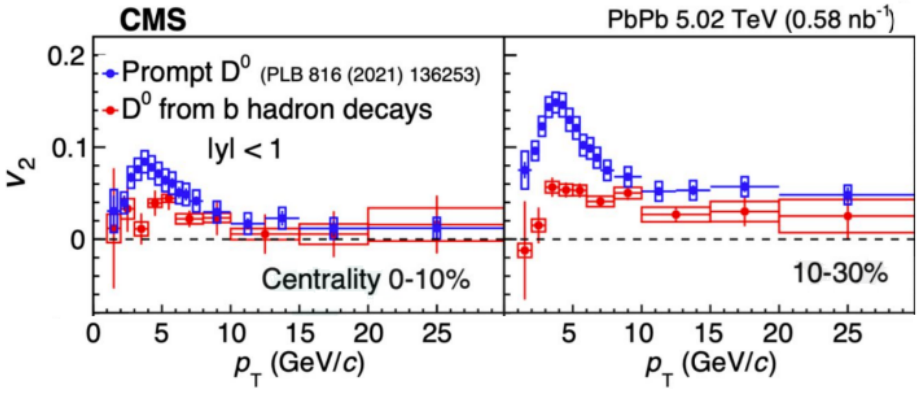

Figure 2: The elliptic flow coefficients of prompt (blue) [10] and non-prompt (red) [9] D^0 mesons vs p_T.

inherently weaker. The elliptic flow measurements from LHCb are also compared with predictions from the AMPTmodel [8] that incorporates string melting to simulate the dense partonic matter and employs quark coalescence as a mechanism for particle production. While the model captures the overall trend, it overestimates the elliptic flow at low transverse momentum (p_T). The collective motion of heavy-flavor quarks, such as charm and beauty, have been investigated through the measurement of anisotropies in heavy-flavor hadron production. Fig. 2 presents the elliptic flow coefficients measured by the CMS Collaboration for prompt and non-prompt D-mesons across two centrality ranges [9]. The results reveal a significant elliptic flow for both charm and beauty hadrons, underscoring the participation of heavy flavors in the medium collective motion. A clear mass ordering is observed, with the elliptic flow coefficients for heavy-flavor hadrons being smaller than those for particles containing lighter flavors. Additionally, a strong dependence on centrality is evident, with reduced flow observed in more central (symmetric) collisions.

A second key effect of the medium is the energy loss. The particles propagating through it,

PoS(PIC2024)046

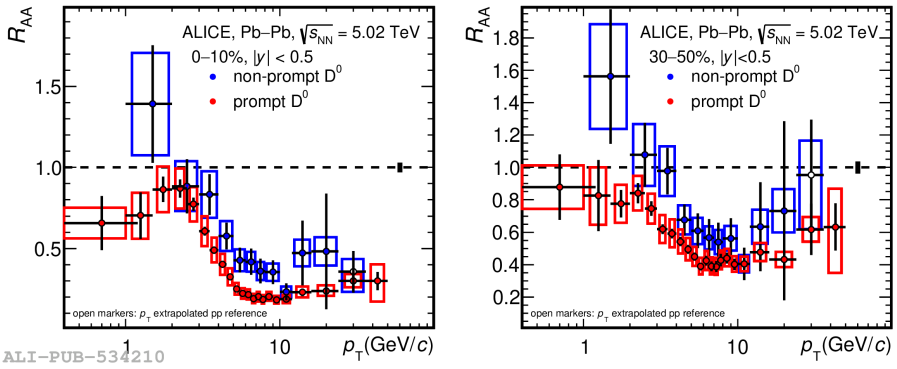

Figure 3: Nuclear modification factor (R_{AA}) of prompt (red) and non-prompt (blue) D^0 mesons in the centrality classes 0–10% (left) and 30–50% (right) [11].

interact with the medium losing energy both via collisional and radiative processes. This in-medium energy loss, which carries information on the medium properties and expansion, can be investigated by measuring the nuclear modification factor, R_{AA}, defined as:

$$R_{AA} = \frac{1}{\langle N_{coll} \rangle} \frac{d^2N_{AA}/dp_T dy}{d^2N_{pp}/dp_T dy} \tag{2}$$

where dN_{AA}/dp_T and dN_{pp}/dp_T are the p_T-differential production yields measured in a given centrality interval in nucleus–nucleus collisions and in pp collisions, respectively and $\langle N_{coll} \rangle$ is the average number of binary nucleon-nucleon collisions in the heavy-ion collision. $R_{AA} \sim 1$ would point to particle yield in heavy-ion collisions consistent with scaled pp results, suggesting no significant medium effects while $R_{AA} < 1$ would indicate a suppression of particle production due to interactions with the dense medium and subsequent energy loss of partons in the QGP. The R_{AA} for prompt and non-prompt D^0 mesons, measured by the ALICE Collaboration, is shown in Fig.3. A pronounced suppression of R_{AA} is observed, indicating significant interactions between heavy quarks and the medium. A larger suppression is observed in central (0-10%) with respect to semi-central (30-50%) collisions. This behavior arises because central collisions create a hotter, denser medium with a longer-lived QGP phase, leading to more pronounced energy loss for quarks traversing the medium. Notably, non-prompt D^0 mesons exhibit less suppression than prompt D^0 mesons, consistent with the expectation that beauty quarks lose less energy than charm quarks due to their larger mass. This behavior aligns with the mass-dependent energy loss trend already seen in the elliptic flow results presented in Fig.2. The comparison between the measured R_{AA} and theoretical models is shown in Fig. 4. The top panel shows that the tested theoretical models describe the experimental data well overall. The bottom panel compares R_{AA} measurements with predictions from the default LGR model [12] and four modified versions. Excluding quark recombination during hadronization (case iv) enhances R_{AA} at $p_T > 1$ GeV/c and reduces it at lower p_T, indicating that the dip in R_{AA} is primarily due to charm-quark coalescence into prompt D^0 mesons. Additionally, replacing the beauty quark mass with the charm quark mass (case i) significantly reduces R_{AA}, highlighting the critical role of heavy-quark mass in energy loss and particle suppression.

Quarkonia, like J/Ψ, are another key probe for studying the QGP. In the QGP, color screening

PoS(PIC2024)046

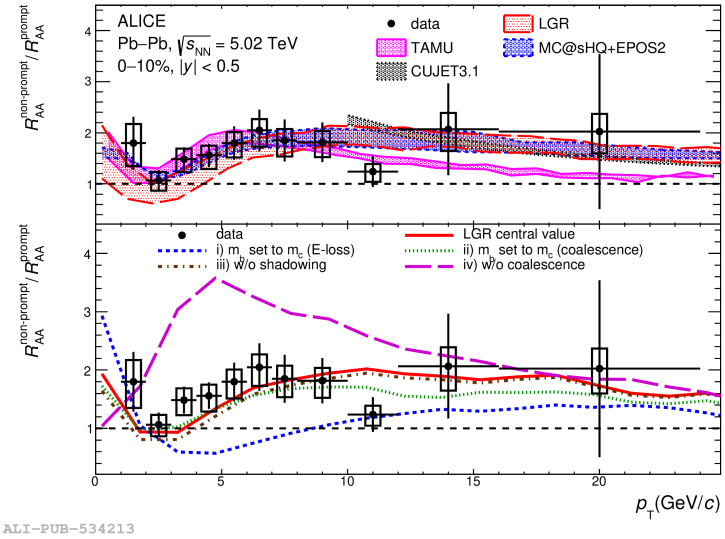

Figure 4: Non-prompt to prompt D^0-meson R_{AA} ratio as a function of p_T in the 0–10% central Pb–Pb collisions at $\sqrt{s_{NN}}$= 5.02, compared to model predictions (top) [12–14], and to different modifications of LGR calculations (bottom) [12].

weakens heavy quark binding, suppressing quarkonium production [15]. Thermal dissociation further contributes to suppression, as the QGP thermal energy can melt pre-formed quarkonium states. Different quarkonium states melt at specific temperatures due to varying binding energies, making them effective QGP thermometers. For example, observing J/Ψ but not excited charmonium states indicates a QGP temperature sufficient to melt the latter but not the J/Ψ ground state. The R_{AA} of the Υ ground state ($\Upsilon(1S)$) and excited states $\Upsilon(2S)$, and $\Upsilon(2S+3S)$ has been measured by the ATLAS Collaboration, as shown in Fig. 5. The left plot presents the R_{AA} as a function of p_T. The results indicate no significant p_T dependence for the suppression; however, a clear hierarchical pattern emerges, with the excited states being more suppressed than the ground state. This behavior reflects the progressive melting of quarkonium states in the QGP, driven by their different binding energies. For all three states, the R_{AA} value decreases with increasing centrality (right plot in Fig. 5), indicating that higher temperatures are reached in more central collisions. Additionally, the measured suppression is compared with the model by Du et al. [16], which incorporates color screening, regeneration, and temperature-dependent binding energy. The model provides an excellent description of the suppression observed for all three quarkonium states, capturing the measured trends.

Jet-related observables also provide valuable insights into QGP properties. The parton shower differs significantly between vacuum and medium environments. In the medium, partons lose energy, as shown by R_{AA} measurements (Figs. 3 and 5), and experience directional changes due to interactions with medium constituents. These changes can be examined by measuring the angle between leading and recoil jets in pp (typically back-to-back) and heavy-ion collisions. The angular dependence of jet production, measured by the ALICE Collaboration [18], is shown in Fig. 6 for two different recoil jet p_T ranges. In the lower panels, the nuclear modification factor I_{AA}, defined as the ratio of the distributions in Pb-Pb to those in pp collisions, is presented. For high-p_T jets (right

PoS(PIC2024)046

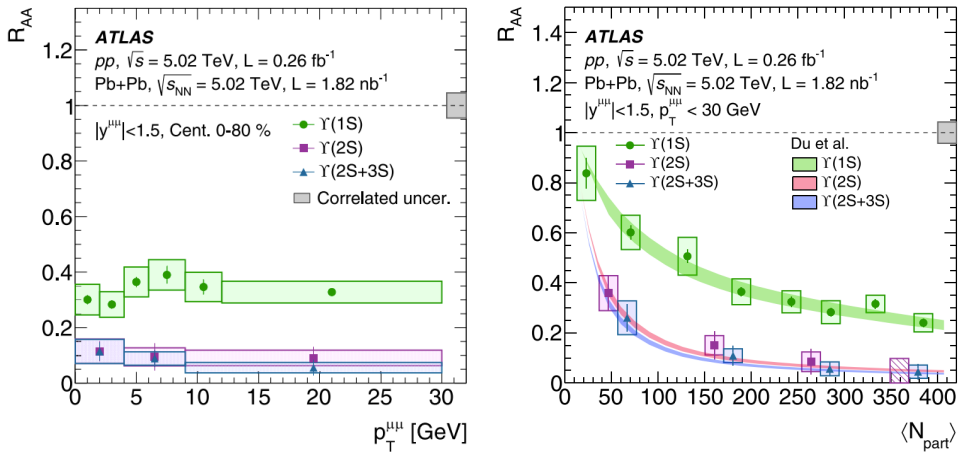

Figure 5: The nuclear modification factor of $\Upsilon(1S)$, $\Upsilon(2S)$, and $\Upsilon(2S+3S)$ as function of p_{T} (left) and centrality (right) at 5.02 TeV [17]. The R_{AA} vs centrality is compared with the model by Du et al [16].

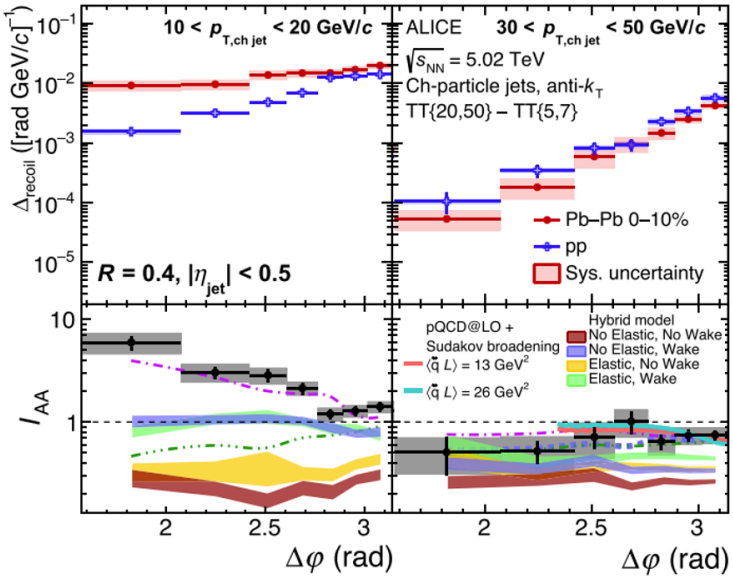

Figure 6: Upper panels: corrected recoil jet distributions in Pb-Pb and pp collisions at 5.02 TeV as a function of the angle between the leading and the recoil jet, for intervals in recoil jet p_{T}: [10,20] (left), and [30,50] (right) GeV/c [18]. Lower panels: Comparison of the measured I_{AA} with theoretical predictions [19–21].

panel), a strong medium-induced yield suppression ($I_{AA} < 1$) is observed. In contrast, low-p_{T} jets exhibit a marked medium-induced excess ($I_{AA} > 1$), which increases with greater deviation of the angle $\Delta\phi$ from π. This excess can be explained by the broadening of the recoil jet. Furthermore, the I_{AA} is compared with several theoretical models. Only the JEWELS model [19], which accounts for both collisional and radiative parton energy loss mechanisms, is able to simultaneously describe the jet broadening and suppression.

PoS(PIC2024)046

3. Exploring new physics with ultra-peripheral collisions

While Pb–Pb collisions at LHC are primarily performed to investigate the properties of the QGP, they also provide access to an entirely different regime of physics through UPCs. In UPCs, the nuclei pass close to each other without direct hadronic interactions, allowing their strong electromagnetic fields to drive photon-photon and photon-nucleus processes. Unlike central Pb–Pb collisions, UPCs create a clean experimental environment with minimal background, making them ideal for studying rare phenomena and searching for new physics beyond the Standard Model. The ATLAS Collaboration has, for instance, investigated the possible production of magnetic monopoles [22]. The interaction of strong electromagnetic fields in UPCs can lead to the production of magnetic monopole-antimonopole pairs via the photon-photon fusion process $\gamma \rightarrow M\bar{M}$. Once produced, magnetic monopoles would behave as highly ionizing particles, characterized by their unique straight trajectories through the detector. The analysis relies on the properties of clusters of hits in the innermost layers of the ATLAS silicon detector. Monopoles produce highly collimated hit clusters, forming patterns consistent with straight trajectories, distinguishing them from background signals. To enhance the discrimination between monopoles and beam-induced background, a variable called *transverse thrust (T)* is defined:

$$T = \frac{1}{n_{PixCl}} \sum_{i=1}^{n_{PixCl}} |\hat{r_i} \times \hat{n}| \tag{3}$$

where $\hat{r_i}$ is the direction of a given pixel cluster in the transverse plane with respect to the origin of the ATLAS coordinate system, and the transverse direction $\hat{n}$ maximizes the expression. The T variable has a maximum value of 1, corresponding to a set of fully aligned pixel clusters, and a minimum value of approximately $2/\pi$, which occurs for a uniform distribution of clusters in the transverse plane. Simulated signal events, representing the trajectories of monopoles, typically yield T values close to unity. Based on these simulated signal properties, a selection criterion of $T > 0.95$ is applied to define the signal region (SR), effectively distinguishing potential monopole events from the background. The measured T distribution is shown in the left panel of Fig 7. The number of signal events found (3) is consistent with the expected background. While no evidence for magnetic monopoles was found, the analysis sets an upper limit on the monopole production cross-section, reported on the right panel of Fig 7. This result significantly improves upon the previous limits reported by the MoEDAL experiment [23].

4. Conclusions

In this contribution, several observables have been discussed to highlight the progress in probing the quark-gluon plasma in heavy-ion collisions at the LHC. Collective motion provides insight into the hydrodynamic behavior of the medium. The study of partons energy loss, through measurements of the nuclear modification factor, and the recoil jet deflection, further reveals the QGP interactions with the partons. Quarkonia suppression in excited states continues to be a powerful signature of QGP deconfinement, offering valuable insights into the medium temperature. In addition to these QGP-related probes, ultra-peripheral collisions provide a unique opportunity to explore new physics phenomena, as the ATLAS search for magnetic monopoles. The heavy-ion

PoS(PIC2024)046

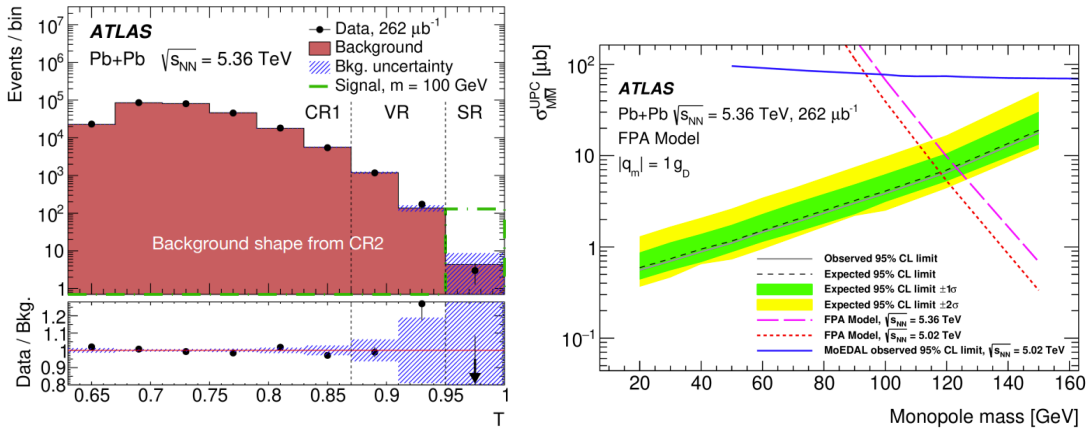

Figure 7: Left: T distribution for data (markers) [22] and the estimated background (filled histograms). Right: upper limits on the monopole pair production cross-section in Pb+Pb UPC at 5.36 TeV. The limits are compared with the measurement by MoEDAL at 5.02 TeV [23].

program at the LHC is set to enter an exciting new phase with the data-taking campaigns of LHC Run 3 and Run 4. Comprehensive upgrades across all major LHC experiments will enable more precise and detailed measurements, enhancing the study of QGP properties and expanding the scope of the physics program.

References

[1] **ATLAS** Collaboration, "The atlas experiment at the cern large hadron collider," *Journal of Instrumentation* **3** no. 08, (Aug, 2008) S08003.

[2] **CMS** Collaboration, "The cms experiment at the cern lhc," *Journal of Instrumentation* **3** no. 08, (Aug, 2008) S08004.

[3] **ALICE** Collaboration, "The alice experiment at the cern lhc," *Journal of Instrumentation* **3** no. 08, (Aug, 2008) S08002.

[4] **LHCb** Collaboration, "The lhcb detector at the lhc," *Journal of Instrumentation* **3** no. 08, (Aug, 2008) S08005.

[5] **ATLAS** Collaboration, "Measurement of the azimuthal anisotropy of charged particles produced in $\sqrt{s_{\rm NN}}$= 5.02tev pb+pb collisions with the atlas detector," *The European Physical Journal C* **78** no. 997, (2018) .

[6] **ALICE** Collaboration, "Energy dependence and fluctuations of anisotropic flow in pb-pb collisions at $\sqrt{s_{\rm NN}}$ = 5.02 and 2.76 tev," *Journal of High Energy Physics* no. 103, (2018) .

[7] **LHCb** Collaboration, "Measurement of forward charged hadron flow harmonics in peripheral pbpb collisions at $\sqrt{s_{NN}}$ = 5.02 TeV with the lhcb detector," *Phys. Rev. C* **109** (May, 2024) 054908.

PoS(PIC2024)046

[8] Z. Lin and L. Zheng, "Further developments of a multi-phase transport model for relativistic nuclear collisions," *Nuclear Science and Techniques* **32** no. 113, (2021) .

[9] **CMS** Collaboration, "Measurements of azimuthal anisotropy of nonprompt d0 mesons in pbpb collisions at snn=5.02tev," *Physics Letters B* **850** (2024) .

[10] **CMS** Collaboration, "Measurement of prompt d0 and d0 meson azimuthal anisotropy and search for strong electric fields in pbpb collisions at snn=5.02tev," *Physics Letters B* **816** (2021) 136253.

[11] **ALICE** Collaboration, "Measurement of beauty production via non-prompt d0 mesons in pb-pb collisions at $\sqrt{s_{\rm NN}}$= 5.02 tev," *Journal of High Energy Physics* **2022** (2022) .

[12] L. Shuang and L. Jinfeng, "Data-driven extraction of heavy quark diffusion in quark-gluon plasma," *The European Physical Journal C* **80** no. 671, (2020) .

[13] M. He, R. J. Fries, and R. Rapp, "Heavy flavor at the large hadron collider in a strong coupling approach," *Physics Letters B* **735** (2014) 445–450.

[14] M. Nahrgang, J. Aichelin, P. B. Gossiaux, and K. Werner, "Influence of hadronic bound states above T_c on heavy-quark observables in pb + pb collisions at the cern large hadron collider," *Phys. Rev. C* **89** (Jan, 2014) 014905.

[15] **ALICE** Collaboration, "Prompt and non-prompt j/ψ production at midrapidity in pb–pb collisions at $\sqrt{s_{\rm NN}}$= 5.02 tev," *Journal of High Energy Physics* **2024** (2024) .

[16] X. Du, M. He, and R. Rapp, "Color screening and regeneration of bottomonia in high-energy heavy-ion collisions," *Phys. Rev. C* **96** (Nov, 2017) 054901.

[17] **ATLAS** Collaboration, "Production of $\Upsilon(ns)$ mesons in Pb + Pb and pp collisions at 5.02 tev," *Phys. Rev. C* **107** (May, 2023) 054912.

[18] **ALICE** Collaboration, "Observation of medium-induced yield enhancement and acoplanarity broadening of low-$p_{\rm t}$ jets from measurements in pp and central pb-pb collisions at $\sqrt{s_{\rm NN}}$ = 5.02 TeV," *Phys. Rev. Lett.* **133** (Jul, 2024) 022301.

[19] K. Zapp, "Jewel 2.0.0: directions for use," *The European Physical Journal C* **74** (2014) .

[20] **JETSCAPE** Collaboration, "Inclusive jet and hadron suppression in a multistage approach," *Phys. Rev. C* **107** (Mar, 2023) 034911.

[21] J. Brewer, Q. Brodsky, and K. Rajagopal, "Disentangling jet modification in jet simulations and in Z+jet data," *JHEP* **02** (2022) 175, arXiv:2110.13159 [hep-ph].

[22] **ATLAS** Collaboration, "Search for magnetic monopole pair production in ultraperipheral pb+pb collisions at $\sqrt{s_{\rm NN}}$ = 5.36 tev with the atlas detector at the lhc," 2024. https://arxiv.org/abs/2408.11035.

[23] **MoEDAL** Collaboration, "j/ψ production versus centrality, transverse momentum, andrapidity in Au + Au collisions at $\sqrt{s_{NN}}$ = 200 GeV," *Nature* **602** (2022) .

PoS(PIC2024)046